

EPFL

■ École
polytechnique
fédérale
de Lausanne

Institute of Materials - Institute of Bioengineering
sunmil.epfl.ch

SuNMIL

■ Supramolecular
NanoMaterials
and Interfaces
Laboratory

Catalysis on Surfaces

Lesson 14

MSE 304

Francesco Stellacci

桑繆 썬밀 सानमिल ΣουΝΜΙΛ سنمیل CaHMPЛ



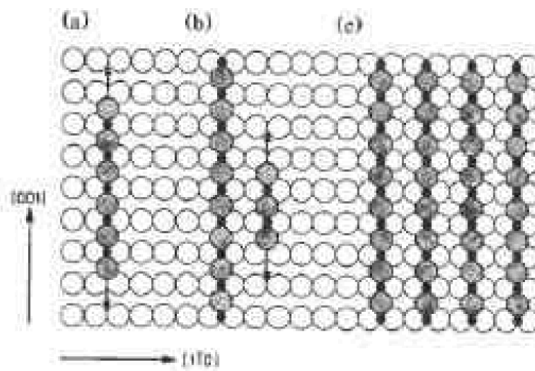
Reading for this Class

Reviews by Nørskov

Key Topics from the Previous Class

Absorption at Interfaces

Absorption at Interfaces – Effect of Surface Coverage



(2x1)-O/Cu(110)

Absorption at Interfaces – Surface “Softness

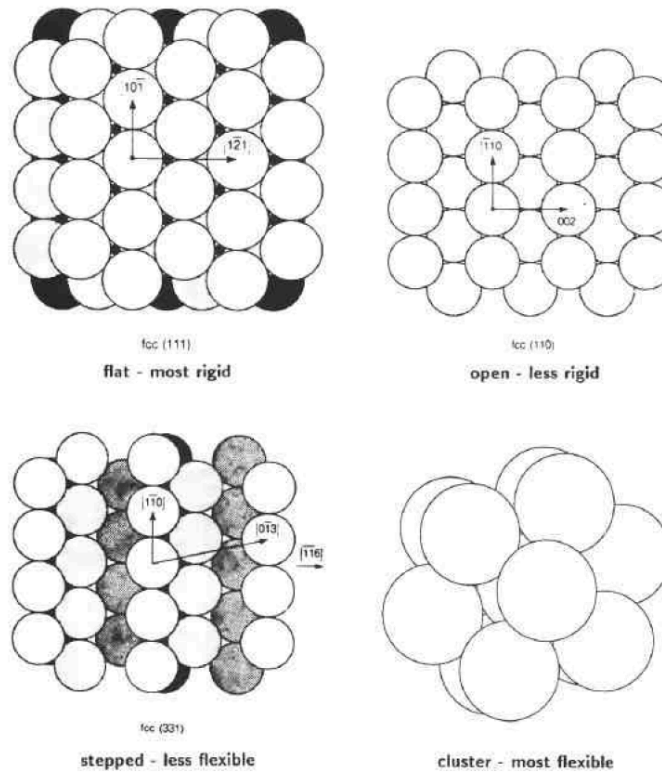


Figure 6.12. Models of surfaces divided according to their atom coordination. Atoms in the close-packed (111) surfaces of fcc metals have the highest coordination, their relaxation is small, and chemisorption-induced restructuring is most difficult. These we call *rigid surfaces*. Clusters have the lowest coordination accompanied by large relaxation and thermodynamically favorable chemisorption-induced restructuring; these are the most flexible. The more open fcc (110) surface and stepped surfaces show intermediate flexibility [29].

What is Catalysis?

Why Surfaces can be Catalysts?

The Molecular Orbital Theory

Bonding at Surfaces

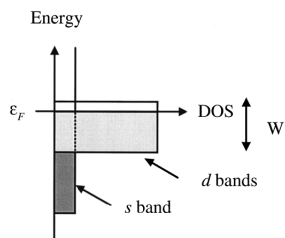


FIG. 2. Schematic illustration of the density of states of a transition metal, showing the broad *s* band and the narrow *d* bands (width W) around the Fermi level, ε_F .

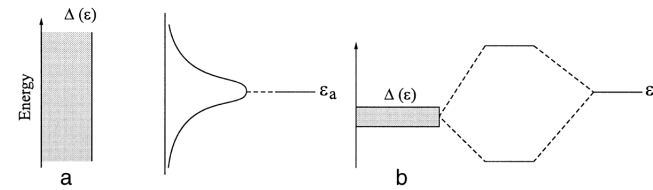


FIG. 3. The local density of states at an adsorbate in two limiting cases: (a) for a broad surface band; (b) for a narrow metal band. Case a corresponds to the interaction with a metal *s* band and case b is representative of the interaction with a transition metal *d* band.

Bonding at Surfaces – Strength of Bonding

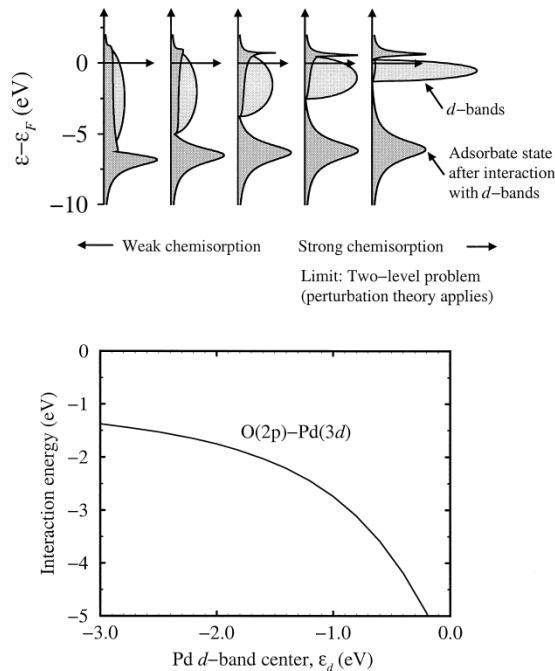


FIG. 4. The local density of states projected onto an adsorbate state interacting with the d bands at a surface. The strength of the adsorbate–surface coupling matrix element V is kept fixed as the center of the d bands ε_d is shifted up toward the Fermi energy ($\varepsilon_F = 0$) and the width W of the d bands is decreased to keep the number of electrons in the bands constant. As ε_d shifts up, the antibonding states are emptied above ε_F and the bond becomes stronger (bottom). The calculation was done by using the Newns–Anderson model (37). Adapted from Hammer (38).

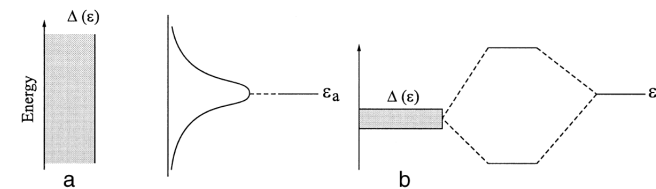


FIG. 3. The local density of states at an adsorbate in two limiting cases: (a) for a broad surface band; (b) for a narrow metal band. Case a corresponds to the interaction with a metal s band and case b is representative of the interaction with a transition metal d band.

O in a p(2X2) layer on Pt(111)

Bonding at Surfaces – Strength of Bonding

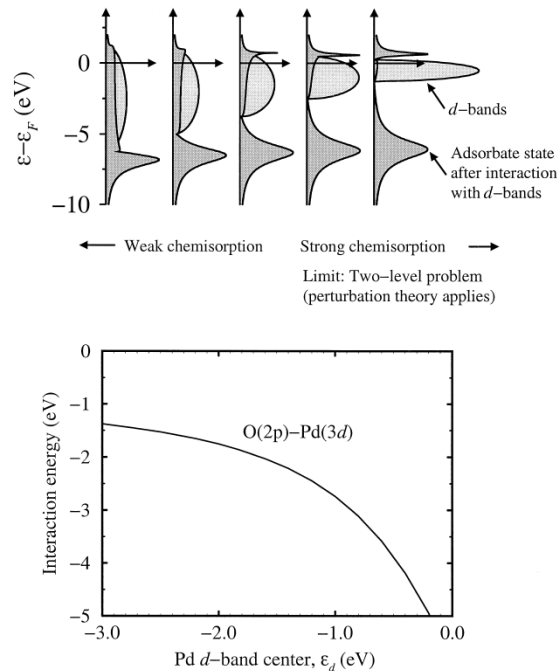


FIG. 4. The local density of states projected onto an adsorbate state interacting with the d bands at a surface. The strength of the adsorbate–surface coupling matrix element V is kept fixed as the center of the d bands ε_d is shifted up toward the Fermi energy ($\varepsilon_F = 0$) and the width W of the d bands is decreased to keep the number of electrons in the bands constant. As ε_d shifts up, the antibonding states are emptied above ε_F and the bond becomes stronger (bottom). The calculation was done by using the Newns–Anderson model (37). Adapted from Hammer (38).

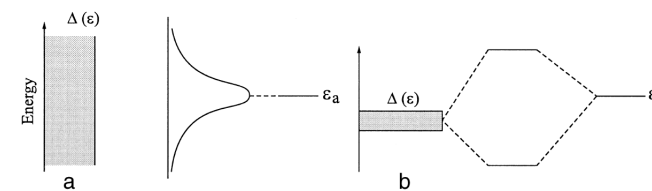


FIG. 3. The local density of states at an adsorbate in two limiting cases: (a) for a broad surface band; (b) for a narrow metal band. Case a corresponds to the interaction with a metal s band and case b is representative of the interaction with a transition metal d band.

O in a p(2X2) layer on Pt(111)

Bonding at Surfaces – The Antibonding Molecular States

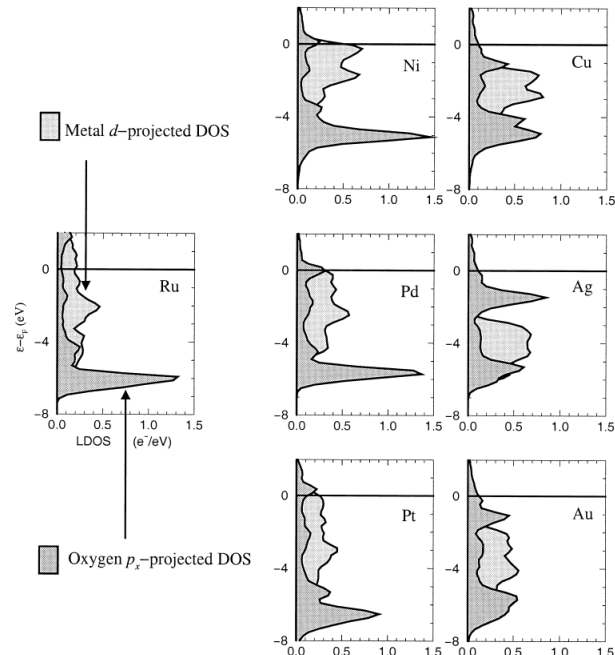


FIG. 7. Local density of states projected onto the oxygen $2p_x$ state (dark-shaded area) for atomic oxygen 1.3 Å above close-packed surfaces of late transition metals (cf. Fig. 6). The light-shaded areas give the metal d -projected DOS for the respective metal surfaces before the oxygen chemisorption. From Hammer and Nørskov (40).

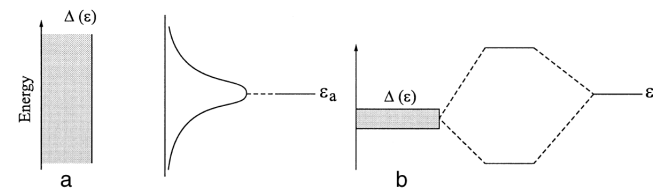


FIG. 3. The local density of states at an adsorbate in two limiting cases: (a) for a broad surface band; (b) for a narrow metal band. Case a corresponds to the interaction with a metal s band and case b is representative of the interaction with a transition metal d band.

The Chemical Bond

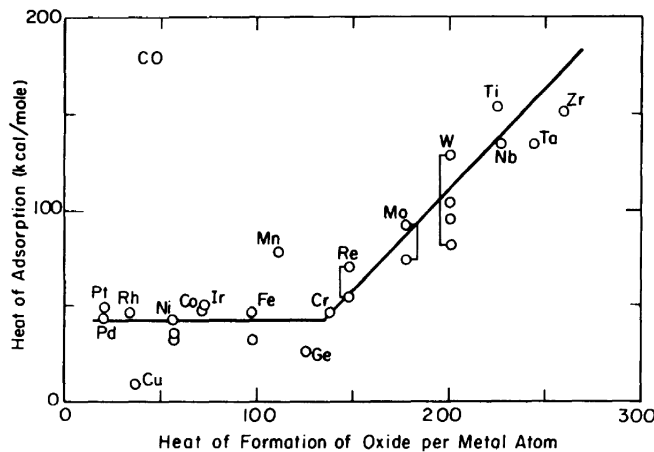


Figure 6.3. Heats of adsorption of CO on various transition metals as a function of the heats of formation of the corresponding oxides (per metal atom) [2].

The Chemical Bond

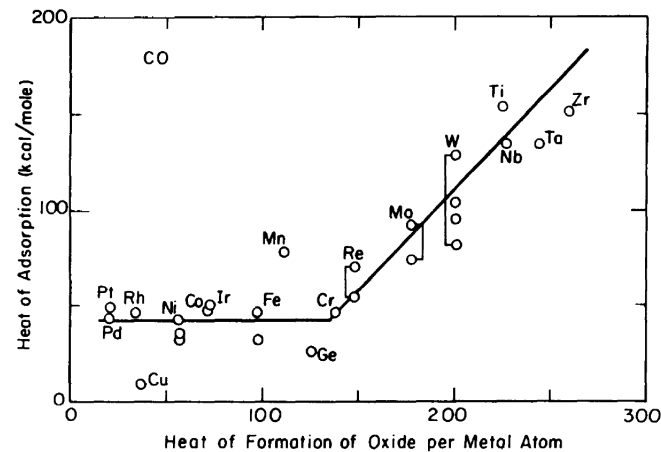


Figure 6.3. Heats of adsorption of CO on various transition metals as a function of the heats of formation of the corresponding oxides (per metal atom) [2].

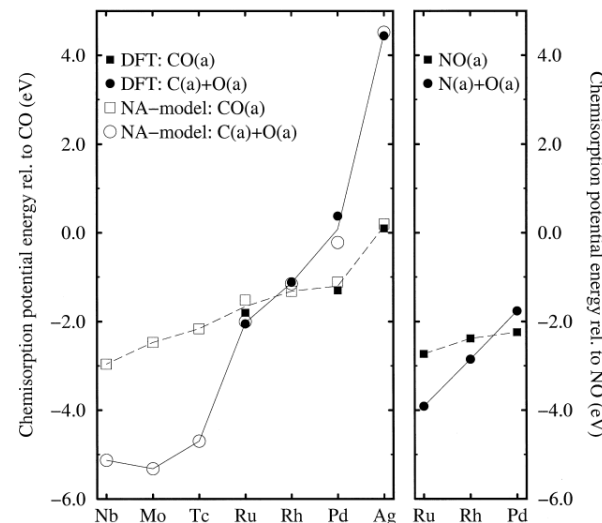


FIG. 13. (Left) Calculated (PW91) and model estimates of the variation in the adsorption energy of molecular CO compared to atomically adsorbed C and O for the most close-packed surface of the 4d transition metals. (Right) Calculated (PW91) molecular and dissociative chemisorption of NO. Solid symbols are DFT calculations; open symbols are Newns–Anderson model calculations. For CO, dissociative chemisorption appears to the left of rhodium. For NO, dissociative chemisorption appears farther to the right, i.e., also on rhodium.

Dissociative Absorption at Surfaces

CO

Sc	Ti D	V	Cr	Mn	Fe D	Co	Ni M	Cu
Y	Zr	Nb	Mo D	Tc	Ru M	Rh	Pd M	Ag
La	Hf	Ta	W D+M	Re	Os	Ir M	Pt M	Au

3d
4d
5d

N₂

Sc	Ti (D)	V	Cr (D)	Mn	Fe D	Co	Ni	Cu
Y	Zr	Nb	Mo (D)	Tc	Ru	Rh	Pd	Ag
La	Hf	Ta	W (D)	Re	Os	Ir	Pt	Au

3d
4d
5d

NO

Sc	Ti	V	Cr	Mn	Fe	Co	Ni D+M	Cu
Y	Zr	Nb	Mo	Tc	Ru M	Rh	Pd M	Ag
La	Hf	Ta	W	Re	Os	Ir D+M	Pt M	Au

3d
4d
5d

FIG. 14. Compilation of experimental data for the ability of transition metals to adsorb and dissociate CO, N₂, and NO molecules. M, molecular adsorption; D, dissociative adsorption. Adapted from Broden *et al.* (57).

Catalysis at Surfaces

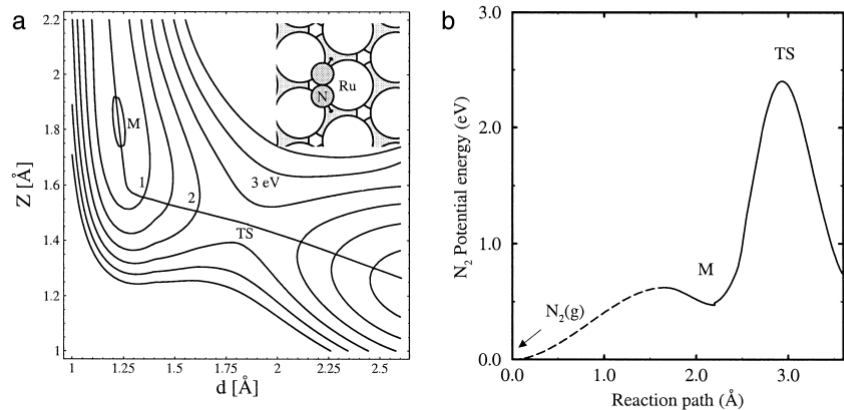


FIG. 19. (a) The potential energy surface (RPBE) for N_2 dissociating on a Ru(0001) surface. The energy zero is a molecule far from the surface. The adsorption geometry is shown in the inset. The distance of the center of mass of the molecule above the surface, Z , and the N–N bond length, d , are varied. The minimum energy path is indicated, and in (b) the energy along the path is shown. Note that here only two degrees of freedom have been included. When the rest are included, the minimum energy path has a lower energy barrier (Fig. 34). Adapted from Murphy *et al.* (71).

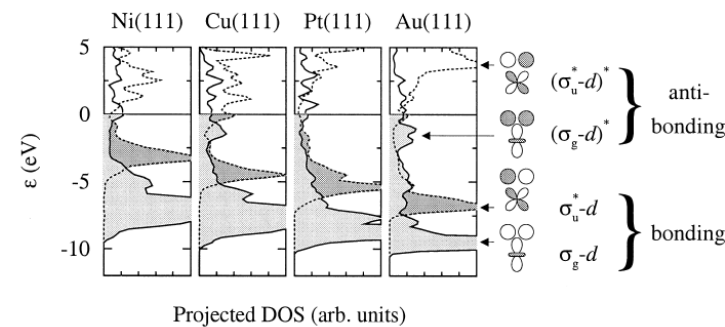
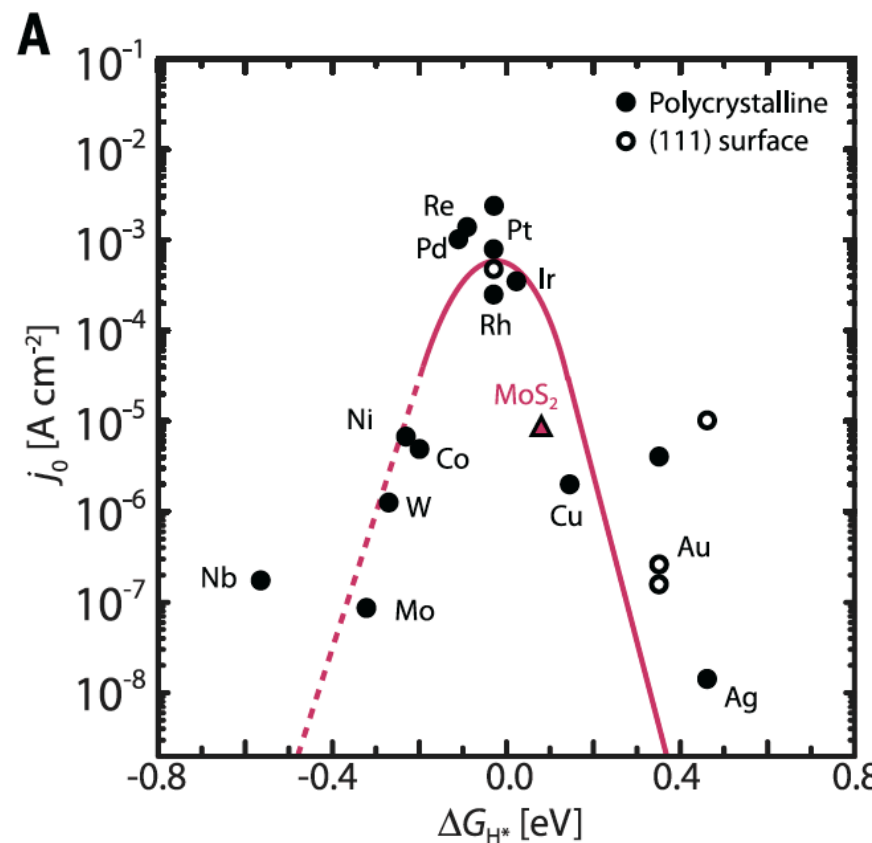


FIG. 21. The DOS projected onto σ_g and σ_u^* for H_2 in the dissociation transition state on Cu(111), Ni(111), and Au(111), and Pt(111) surfaces. From Hammer and Nørskov (40).

The Sabatier Principle



Real Surfaces: Strain

Real Surfaces: TLK

Real Surfaces: Edges

Catalyst Poisoning

Catalyst Regeneration

Real Surfaces: Frontier Research

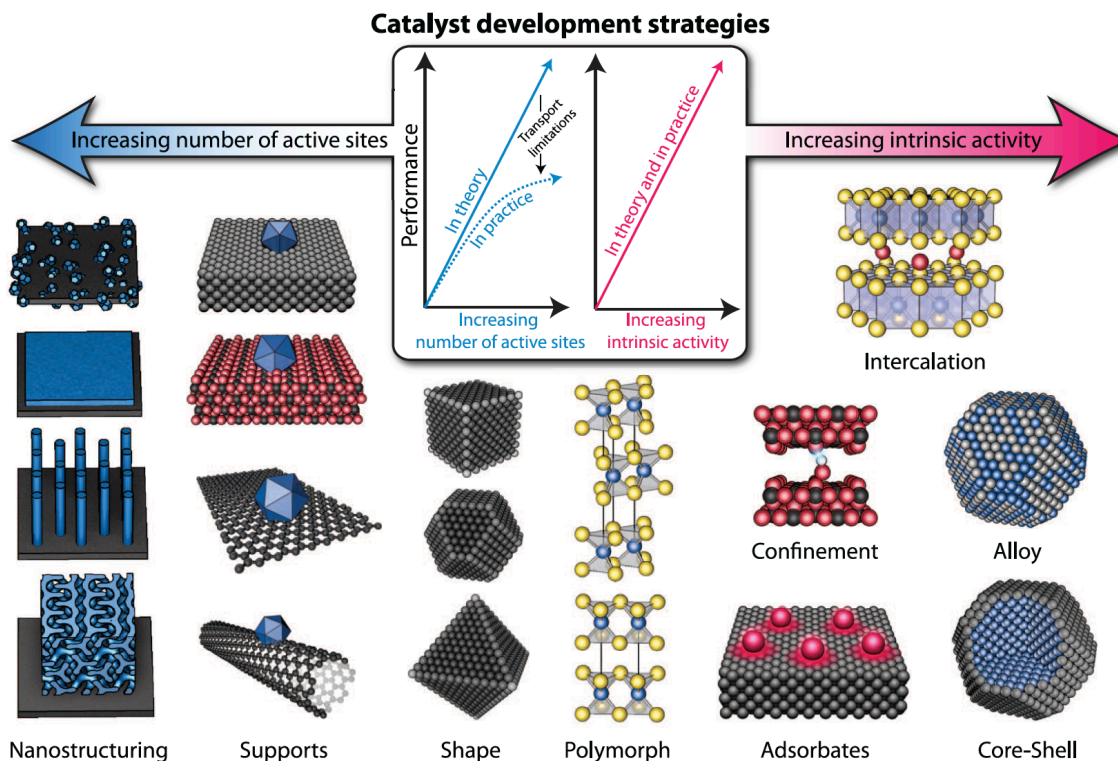


Fig. 2. Catalyst development strategies. Schematic of various catalyst development strategies, which aim to increase the number of active sites and/or increase the intrinsic activity of each active site.

Why is this Important

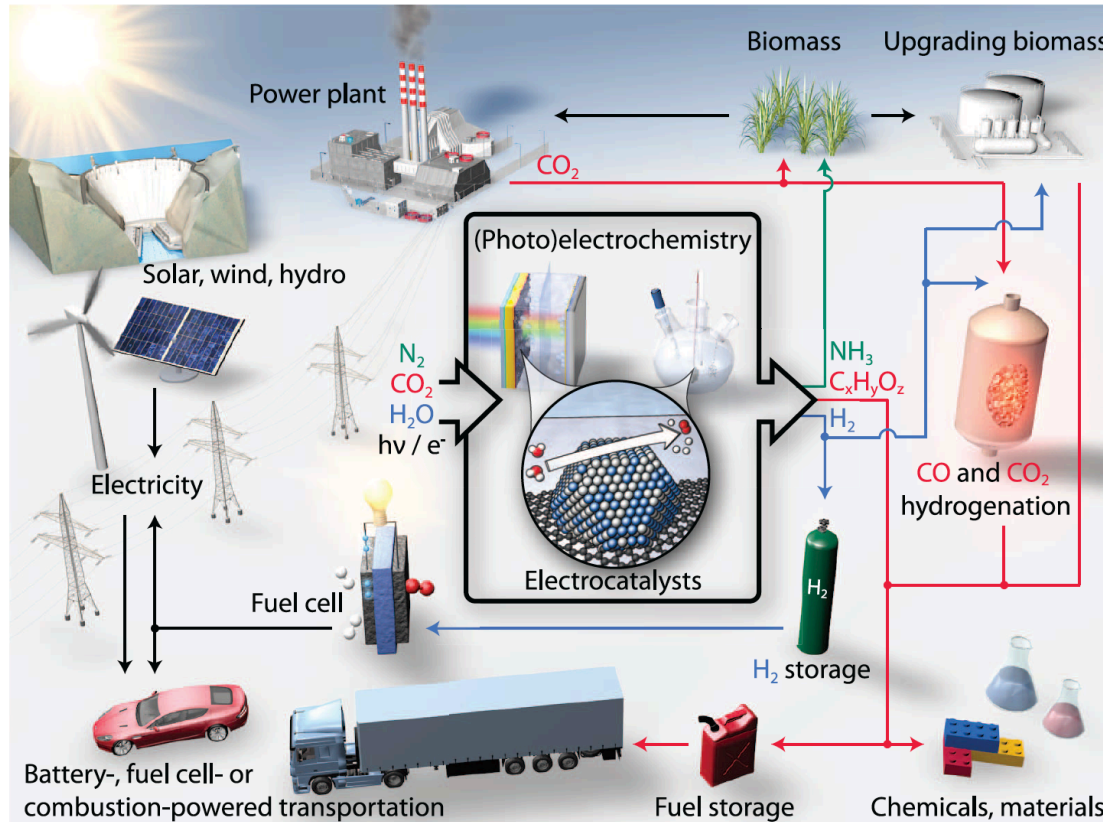


Fig. 1. Sustainable energy future. Schematic of a sustainable energy landscape based on electrocatalysis.

Selective Catalysts

Conclusions
